Excitons with large binding energies in MgS/ZnSe/MgS and ZnMgS/ZnS/ZnMgS quantum wells

2001 J. Phys.: Condens. Matter 13 2317

(http://iopscience.iop.org/0953-8984/13/10/322)

INSTITUTE OF PHYSICS PUBLISHING JOURNAL OF PHYSICS: CONDENSED MATTER

J. Phys.: Condens. Matter **13** (2001) 2317–2329 www.iop.org/Journals/cm PII: S0953-8984(01)17747-7

Excitons with large binding energies in MgS/ZnSe/MgS and ZnMgS/ZnS/ZnMgS quantum wells

B Urbaszek[1], C Morhain[1], C Bradford[1], C B O'Donnell[1], S A Telfer[1], X Tang[1], A Balocchi[1], K A Prior[1], B C Cavenett[1], C M Townsley[2] and R J Nicholas[2]

[1] Department of Physics, Heriot-Watt University, Edinburgh EH14 4AS, UK
[2] Clarendon Laboratory, Department of Physics, University of Oxford, Parks Road, Oxford OX1 3PU, UK

Received 4 October 2000, in final form 17 January 2001

Abstract

The wide bandgap II–VI semiconductors have unique properties which allow the possibility of suppressing the exciton–phonon scattering up to room temperature in quantum well structures designed so that the exciton excitation $E_{1s\rightarrow 2s} > h\nu_{LO}$. In particular, magnetic field and temperature dependent measurements are used to study the exciton binding energies and to investigate the exciton–LO phonon scattering processes of high quality ZnSe quantum wells in MgS grown by MBE. The small inhomogeneous broadening of the exciton transitions in these samples allows the observation of higher excited exciton states. Due to the large difference in band gap between ZnSe and MgS the exciton binding energy in a 5 nm well is found to be 43.9 meV, which is the largest reported for this material system. The FWHM of the heavy hole absorption transitions measured as a function of temperature shows that the scattering of the excitons by the LO phonons is partially suppressed. These results are compared with ZnS quantum wells where the exciton g-values have been measured and the exciton binding energies have been deduced from the exciton diamagnetic shifts. The results show the possibility of suppressing exciton–LO phonon scattering in these structures.

1. Introduction

When a wide bandgap semiconductor is excited optically, the electrons and photogenerated holes are bound strongly together as excitons by the Coulombic interaction. Devices based on these materials are useful only if these excitons are stable at room temperature. However, the strong interaction between the excitons and lattice vibrations (phonons) usually results in the dissociation of the excitons, reducing device efficiencies, and so it is important to explore specific semiconductor microstructures to demonstrate the suppression of longitudinal optical (LO) phonon scattering. It is well documented that the ability to stabilize excitons at room

temperature by the suppression of the exciton–LO phonon scattering is a key factor for high performance optoelectronic devices. For example, in the case of modulators, an enhancement of the excitonic absorption and the narrowing of the linewidth at room temperature are expected, whereas for lasers, excitonic gain is much higher than that associated with a free electron–hole plasma and should allow low threshold laser emission [1]. This is in agreement with recent studies which have predicted that a very high gain, at least 50 times more than that determined in usual III–V or II–VI laser structures, could be obtained in ZnSe QWs up to 150 K [2].

The suppression of the exciton–LO phonon scattering should occur when the energy difference between the ground state and the first excited state of the confined exciton is larger than the energy of the LO phonon, namely, $E_{1s\rightarrow 2s} > h\nu_{LO}$, and is due to the absence of final scattering states [3]. It is important to point out at this stage that few *bulk* materials have sufficiently large excitonic binding energies to satisfy this energy condition and, in fact, none among the usual IV–IV, III–V and II–VI semiconductor compounds.

The condition $E_{1s\rightarrow 2s} > h\nu_{LO}$ for exciton–LO phonon scattering suppression is only a first approximation. For a more realistic understanding of the suppression, the exciton–phonon coupling has also to be taken into account explicitly. In fact, in such systems, the exciton–phonon coupling should result in the formation of two entities: firstly, a polaron, which can be observed as an exciton with modified mass and electronic structure, and, secondly, a new quasi-particle known as the *exciton–LO phonon complex* (EPC), which can be regarded as an LO phonon with an acquired electronic structure and modified energies. This complex, predicted theoretically by Toyozawa and Hermanson [4], has rarely been investigated (in comparison with the polaron) and has mainly been studied experimentally in ionic compounds such as CuCl nanocrystals, where the results were not conclusive due to the poor quality of the samples available [5, 6]. In particular, the size distribution of the semiconductor clusters causes an inhomogeneous broadening of the absorption lines which is too large for detailed spectroscopy to be carried out. There is a similar problem with quantum dot systems where there is a distribution of dot sizes. In principle, such broadening effects do not arise for quantum well heterostructures and hence the importance of this approach. Studies of CdTe multiple-quantum-well structures, however, were also inconclusive as in these structures the exciton binding energy was much less than $h\nu_{LO}$ [7].

Large excitonic binding energies compared with that of the LO phonons can be achieved by exciton confinement in a quantum well where there is, of course, the additional advantage of being able to change the exciton binding energy by changing the well width. In this paper we show that $E_{1s\rightarrow 2s} > h\nu_{LO}$ is achievable for both ZnMgS/ZnS/ZnMgS and MgS/ZnSe/MgS quantum well structures. Indeed, in such systems, it becomes possible to tune the free exciton binding energy from smaller to much larger than that of the LO phonons and, most importantly, to explore the resonant conditions when the LO phonon energy is equal to exciton transitions to higher s and p excited states, namely $E_{1s\rightarrow ns,np} = h\nu_{LO}$.

This work shows that exciton–LO phonon suppression is possible in ZnSe and ZnS quantum wells and so provides the foundation for our current studies of the resonant condition and the exciton–phonon complex, the results of which will be published elsewhere.

2. Growth of MgS based quantum wells

MgS is a potentially important wide band gap II–VI compound because in the zincblende (ZB) crystal structure the material has a similar lattice constant to both GaAs and ZnSe, enabling the growth of low strain multilayer structures. In addition, it has a very large band gap and can form an excellent barrier material with good confinement for ZnSe. Unfortunately, the stable bulk crystal structure of MgS is rocksalt (NaCl) and the zincblende structure is metastable

when grown epitaxially on GaAs. Previously, this has severely limited the attempts of various workers to grow layers of MgS of reasonable thickness in the metastable zincblende structure. Teraguchi *et al* [8] were the first to grow ZnSe/MgS superlattices on GaAs substrates by molecular beam epitaxy (MBE) using elemental sources of Mg and S. They observed a clear transition by reflection high energy electron diffraction (RHEED) from 2D growth to 3D as the MgS layer thickness increased. This was attributed to the conversion of the MgS to the NaCl structure and they estimated that the greatest thickness of MgS that could be grown without conversion was 0.96 nm. In addition, the XRD data also showed that the growth of MgS by MBE using elemental sources did not look very promising.

More recently, Uesugi *et al* [9] grew similar ZnSe/MgS superlattices by MOCVD which contained ZB MgS layers up to 10 nm thick. The crystallinity of the MgS layers was sufficiently good to produce high quality MgS/ZnSe multilayers showing large carrier confinement in the ZnSe wells with excitonic emission observed to room temperature [10, 11]. The ZnSe/MgS heterostructures showed a type I band offset, with an estimated band gap for MgS of 5.27–5.47 eV [12]. However, we note that this estimate is much larger than the values for the band gap which have been obtained either by extrapolation of the band gaps of ZnMgSSe alloys [13, 14] or from calculations of the band gap using a modified dielectric theory [14].

We have grown high quality zincblende MgS layers by a novel MBE method using Mg and ZnS as a source of sulphur [15]. Using this technique and growing on a ZnSe/MgS/ZnSe buffer layer, single layers up to 134 nm thick have been produced, together with ZnSe/MgS quantum well structures. All these layers were grown in a Vacuum Generators V80H MBE system using 6 N sources of elemental Zn, Se and Mg together with 6 N ZnS. A liquid nitrogen cooled shutter was used in front of the ZnS cell to prevent contamination of the substrate surface during the thermal clean-up of the substrate. MgS layers were grown at a temperature of 240–270 °C on ZnSe buffer layers deposited in a conventional manner directly on GaAs(001) substrates. On opening the ZnS and Mg shutters, the fluxes reacted at the surface forming MgS and liberating zinc, which did not incorporate substantially into the lattice. A capping layer of ZnSe was necessary to prevent the oxidation of the MgS layer on exposure to air. Double crystal x-ray rocking curves showed that the entire structure exhibited good crystallinity with no evidence of conversion to the NaCl structure and the growth rate of the MgS layer was determined as 0.15 μm h^{-1}. The samples were also examined by SIMS (Loughborough Surface Analysis). Sharp interfaces were observed between the ZnSe and MgS layers and, as expected, a residual Zn signal was found in the MgS layer. The Zn concentration estimated from SIMS measurements is a maximum of 2%, assuming that the sputtering rates for Zn in both the ZnSe and MgS matrices are similar. However, a measurement of the Zn concentration at the surface of the MgS layer was also made by Auger spectroscopy during the SIMS profile and, using this technique, the Zn concentration was estimated to be approximately 0.5%. The lattice constant of a relaxed layer was measured to be 0.5619 ± 0.0001 nm and given that the residual zinc content of the sample lies in the range 0.5–2.0%, we can extrapolate a value for the lattice constant of pure ZB MgS of 0.5622 ± 0.0002 nm. This is slightly larger than the value of 0.559 nm determined from much thinner MgS layers incorporated in ZnSe/MgS superlattices by Uesugi *et al* [9].

A series of ZnSe single quantum well structures were grown of the form ZnSe (buffer)/MgS (barrier)/ZnSe (quantum well)/MgS (barrier)/ZnSe (cap). A summary of the parameters of each sample is given in table 1 and PL from these samples is shown in figure 1. The emission from the barrier could not be observed as the laser excitation energy of 4.5 eV was lower than the band gap of MgS. The PL peaks show large confinement of the heavy hole (HH) excitons and the peak emission energies can be fitted assuming a band gap for MgS of 4.8 eV and a band offset ratio of $\Delta_{CB}/\Delta_{VB} = 1$, shown as the solid line in figure 2. A maximum confinement

Table 1. Parameters for the ZnSe quantum well samples.

	HWA1183 Figure l(a)	HWA1176 Figure 1(b)	HWA1206 Figure 1(c)
Buffer layer thickness (nm)	30	100	25
Well thickness L_w (nm)	10	3.3	1.7
Cap layer thickness (nm)	4.5	3.0	10
PL maximum (eV)	2.821	2.943	3.202
FWHM of PL (meV)	6	17	58

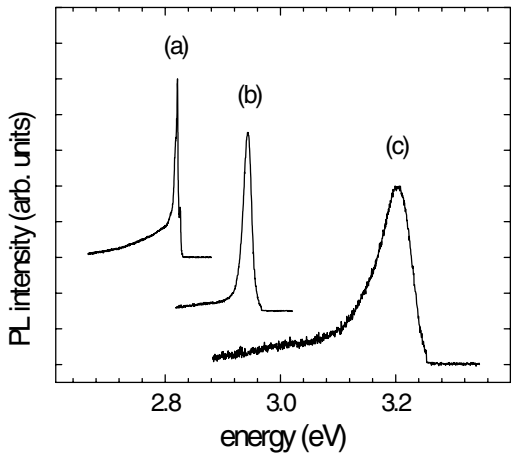

Figure 1. PL of the MgS/ZnSe/MgS quantum well structures with well widths (a) 10 nm, (b) 3.3 nm and (c) 1.7 nm recorded at 5 K using the 275 nm line of an Ar^+ laser.

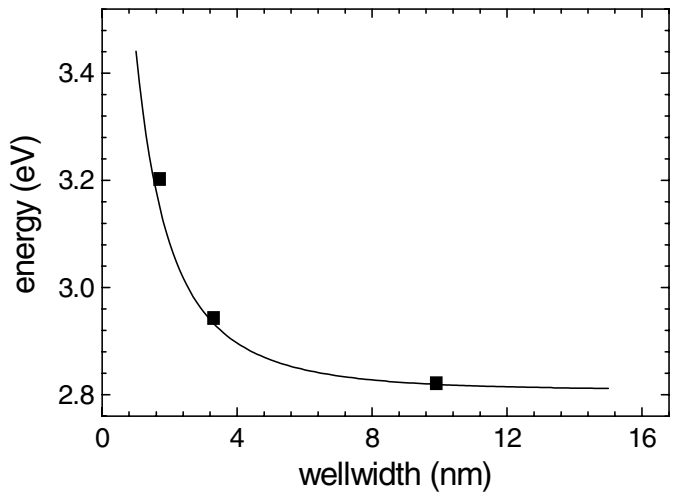

Figure 2. PL emission energies for the same three samples as shown in figure 1. The solid line is a calculated value assuming for MgS $E_g = 4.8$ eV and a band offset ratio of $\Delta_{CB}/\Delta_{VB} = 1$.

of 430 meV was observed for the 1.7 nm well, which we believe is the largest confinement energy measured to date for a ZnSe quantum well and approximates to the case of 2D excitons

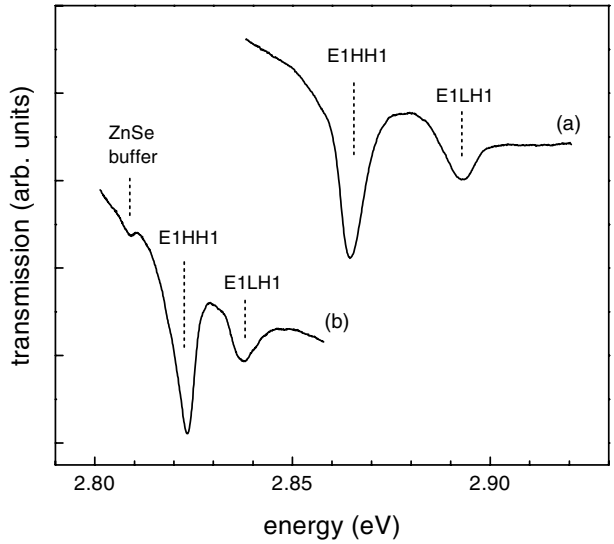

Figure 3. Transmission spectra of MgS/ZnSe/MgS multiple quantum well structures with well widths (a) 5.0 nm and (b) 10.0 nm. For (b) the contribution of the ZnSe buffer appears in the spectrum.

in an infinite well. Values for the measured FWHM of the PL peaks are given in table 1 and it can be seen that the line widths are consistent with the increasing importance of well-width fluctuation as the wells become thinner.

Transmission spectroscopy is a more precise way of measuring the details and widths of the excitonic transitions and so multiple quantum wells are needed in order to have sufficient absorption for these experiments. Two multiple quantum well structures containing ten wells were grown on a ZnSe buffer layer and a thin lattice matched ZnMgSSe cap was added. The high material quality of the two samples reported here is apparent from the transmission spectra at 4 K, shown in figure 3, that were obtained after selectively removing the GaAs substrate by wet etching. The heavy hole exciton (E1HH1) and light hole exciton (E1LH1) ground state transitions are clearly visible for the both the 5.0 nm (a) and 10.0 nm wide quantum wells (b). The FWHMs of the E1HH1 transitions for the 5.0 nm and 10.0 nm quantum well samples are 11.2 meV and 5.8 meV respectively, comparable to values typically obtained for the ZnSe/ZnCdSe and ZnMgSSe/ZnSe quantum wells. The small inhomogeneous broadening indicates only minor well width fluctuations and, in addition, the MgS/ZnSe system with two binary materials has the advantage of minimum alloy broadening.

3. Growth of ZnS based quantum wells

Since the lattice mismatch of ZnS on GaP substrates is only 0.76% and both ZnMgS and ZnCdS can be grown lattice matched to GaP this is an ideal system to explore these new phenomena. The growth of ZnS on GaP using elemental Zn and sulphur supplied from a valved cracker source was described by Ozanyan *et al* [16], while recently Ichino and co-workers have explored the growth of ZnS and related alloy systems using a high flux sulphur cracker in an MBE system which was modified to deal with high sulphur pressures [17–19].

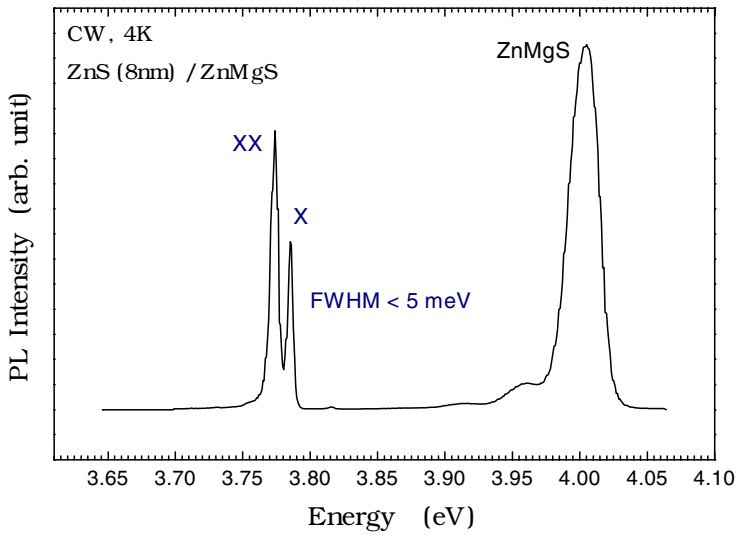

Figure 4. Photoluminescence spectrum taken at 4 K of a ZnMgS/ZnS/ZnMgS quantum well sample with a well width of 8 nm.

All the samples for our investigation were grown using 6 N sources of Zn, Mg and ZnS using standard K-cells. Samples were grown on GaP(100) n^+ substrates and post-growth characterization was carried out by double crystal x-ray diffraction (DCXRD) and PL. The experimental procedure for the growth of optimized ZnS layers in our system has been described in detail previously [20]. The samples were etched *ex situ*, transferred to the MBE system, and the oxide layer was removed between 580 and 630 °C while the sample was exposed to a zinc flux. Using this procedure the (2×4) reconstruction was routinely maintained on cooling the sample to the growth temperature, typically 170 °C. All layers were deposited on a ZnS buffer layer and obtaining a 2D surface on this layer was an important step. To obtain the best surface, at the start of growth, the Zn shutter was closed and the ZnS shutter was opened immediately. Previously, we have deposited a thin layer using only ZnS and then added a small flux from a S cracker to obtain stoichiometric growth conditions, as shown by the appearance of both (2×1) and $c(2 \times 2)$ RHEED patterns. However, even this small flux of sulphur has a detrimental effect on the reproducibility of the sample clean-up and PL quality. Therefore, we currently use no additional sulphur flux for the growth of ZnS or ZnMgS. This has reduced the background pressure from 10^{-8} mbar to typically below 10^{-9} mbar during the removal of the surface oxide and subsequent cooling to the growth temperature.

The PL from ZnS layers grown using only ZnS contains some deep level emission in the range 3.5–3.7 eV, but the spectrum is dominated by a strong donor bound exciton line, I_x. It is thought that in this case the donor is an intrinsic defect such as the sulphur vacancy. Both ZnMgS/ZnS single quantum well and multiple quantum well samples have been grown and the PL from an 8 nm well is shown in figure 4. The spectrum shows both the ZnMgS barrier emission and narrow exciton and biexciton recombinations where the intensity of the latter is consistent with changes of the excitation power and the fact that the emission does not disappear when the temperature is raised up to almost room temperature.

DCXRD spectra are shown in figure 5 for samples containing one 10 nm wide quantum well (curve (a)) and four 4 nm wells with 50 nm ZnMgS barriers (curve (b)). In both samples

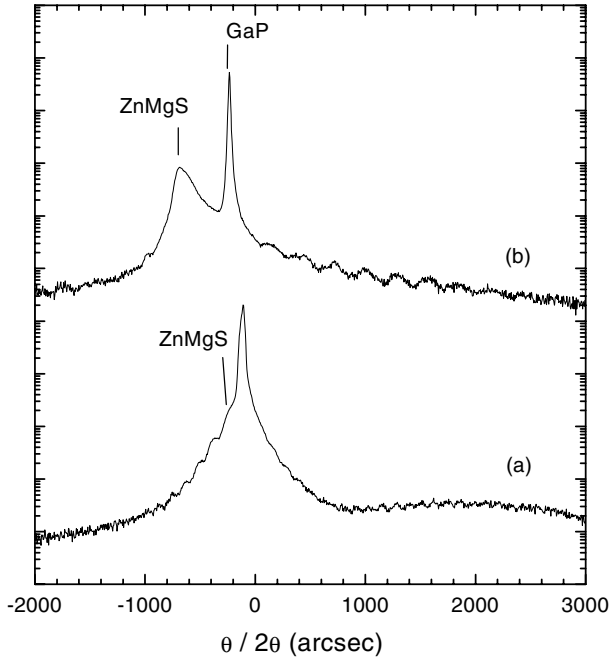

Figure 5. DCXRD spectra for samples with structures (a) ZnMgS (150 nm)/ZnS (10 nm)/ZnMgS (150 nm) and (b) ZnMgS (150 nm)/4 × (ZnS (4 nm) + ZnMgS (50 nm))/ZnMgS (150 nm).

the ZnMgS layer is almost lattice matched to the GaP substrate and in sample (a) the modulation of the rocking curve due to the introduction of a thin layer with a different lattice constant is clearly seen [21–23]. The multi-quantum-well sample (b) also clearly shows the periodicity arising from the combined well and barrier. In both cases the observation of these features is indicative of good crystallinity with sharp interfaces.

4. Magneto-optics of ZnSe

In ZnSe, the bulk exciton binding energy is 20 meV and the LO phonon energy is 32 meV. The band gap for ZnSe is 2.823 eV and for MgS we use 4.8 eV from a fit to the PL data since we have not been able to measure it directly. Since the difference in band gaps is approximately 2 eV, the condition $E^X(1s–2s) > 32$ meV is easily achievable in narrow quantum wells. Also, the large offset for both valence and conduction bands will prevent thermal escape of the carriers from the well to the barrier region.

For a more detailed knowledge of the excitonic properties of the two samples shown in figure 3, the exciton binding energies were measured directly by magneto-transmission, a technique already applied to ZnSe/ZnCdSe by several authors [24]. The large number of ZnSe quantum wells in these MQW structures ensured that the contributions of the cap and buffer regions to the transmission signal were small compared to that of the quantum well transitions. The magneto-optics experiments were carried out at a temperature of 4 K in an Oxford Instruments magnet capable of fields up to 14 T. The spectra were obtained using a halogen lamp as a white light source. The light transmitted through the sample was collected by an optical fibre, dispersed by a 0.75 m single spectrometer equipped with a 1200 lines cm^{-1} grating and recorded using a cooled CCD camera.

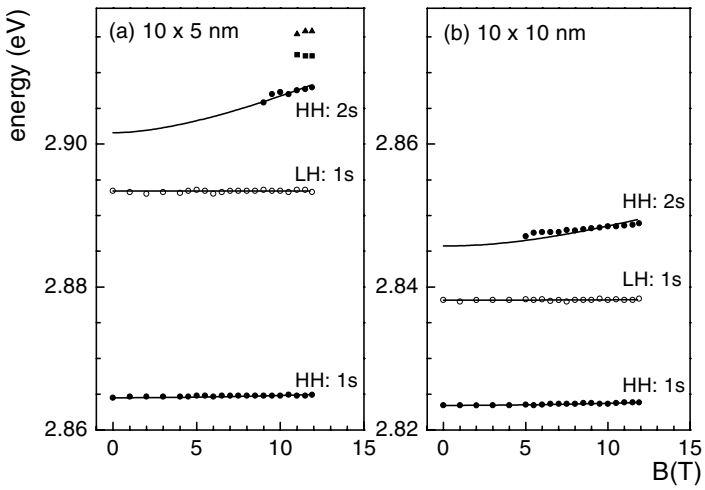

Figure 6. Energy of MgS/ZnSe/MgS exciton transitions at 4 K versus magnetic field as measured by transmission for the two samples shown in figure 3 with well widths (a) 5.0 nm and (b) 10.0 nm. The solid lines are a fit of the data with the model of Engbring and Zimmermann [25].

The higher excited states of the excitons, such as the 2s transitions, are not visible in the zero field transmission spectra, but the oscillator strengths of the higher excited states of the excitons are increased when a magnetic field is applied parallel to the growth direction (Faraday geometry). The transitions are then detectable in the transmission spectra, as shown in figure 6, where the measured energy of the exciton absorption peaks is plotted against the magnetic field strength. The exciton binding energy is obtained by extrapolating the transitions back to the zero field values.

The magneto-exciton transitions are fitted using the model of Engbring and Zimmermann [25] that includes the effects of the confinement potential in the well, the Coulomb interaction and the magnetic field. The 1s exciton states remain nearly unaffected by the magnetic field as the carriers are tightly bound and the Coulomb interaction dominates over the magnetic field effects. For the 5.0 nm and the 10.0 nm wide quantum well samples the 2s HH exciton state emerges at higher fields and the values obtained for the zero field 1s to 2s HH exciton binding energy separations are 22.3 meV for the 10.0 nm well and 37.1 meV for the 5.0 nm well, hence in the latter case the condition $E^X_{HH}(1s–2s) > h\nu_{LO}$ is fulfilled. Also, for the 5 nm well, the corresponding exciton binding energy of 43.9 meV corresponds to a remarkable enlargement by a factor of 2.2 compared with the bulk ZnSe value. This substantial enhancement occurs because of the large difference in band gaps, effectively creating a quantum well with an infinite barrier potential. In fact, our calculations show that for the 1s exciton binding energy tunnelling effects only start to be significant at well widths below one monolayer. In the 10.0 nm wide quantum well the value for the 1s HH exciton binding energy of 28.3 meV is still larger than the bulk value, but the carriers are significantly less confined in this sample. The results are summarized in table 2.

To verify directly the effect of the large exciton binding energy on the stabilization of the exciton at higher temperature the line widths of the heavy hole transitions were measured and the results are given in figure 7, where the FWHM of the HH exciton transitions is plotted versus temperature. The values were obtained from transmission spectra after removing the contributions of the buffer and cap layers. For individual exciton states the broadening can be

Table 2. Parameters for the heavy hole excitons obtained by fitting the magnetic field and temperature dependencies.

Well width (nm)	E^X_{HH}(1s–2s) (meV)	E^X_{HH}(1s) (meV)	Γ_0 (meV)	Γ_{LO} (meV)
5.0	37.1	43.9	(11.0)	(31.8)
10.0	22.3	28.3	6.2	59.0

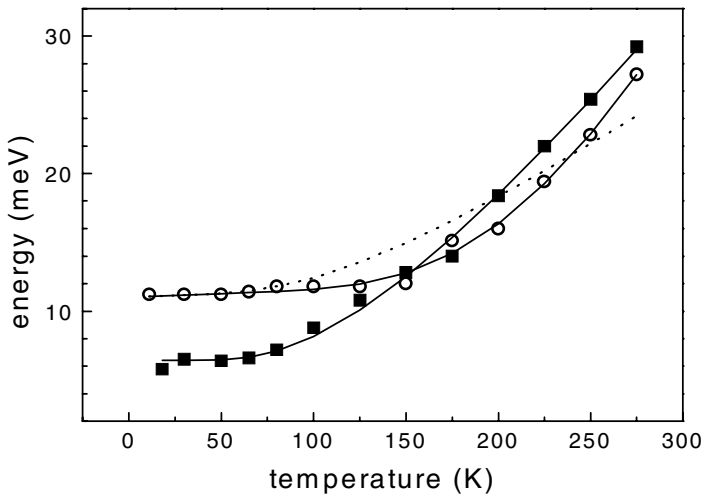

Figure 7. FWHM of the heavy hole exciton transitions versus temperature as measured by transmission and fitted with equation (1) for two samples with ZnSe well widths 5.0 nm (○ and dotted line) and 10.0 nm (■ and solid line). The solid lines through the measured values of the 5.0 nm well illustrates the two regions discussed in the text.

written as

$$\Gamma = \Gamma_0 + \Gamma_{ac}T + \Gamma_{LO}[\exp(h\nu_{LO}/k_BT) - 1]^{-1} \tag{1}$$

where Γ_0 represents the inhomogeneous broadening, Γ_{ac} is the contribution due to the scattering with acoustic phonons and Γ_{LO} is the contribution due to the scattering with LO phonons. The values obtained by fitting the experimental data with (1) are given in table 2. For the fitting procedure, values of 3.0 μeV K^{-1} for the 10.0 nm sample and 5.0 μeV K^{-1} for the 5.0 nm sample were assumed for Γ_{ac}, in accordance with the work of Blewett *et al* [26]. For the 10.0 nm wide quantum well the value for Γ_{LO} of 59.0 meV is very close to that of 60 meV reported for bulk ZnSe [27]. For the 5.0 nm wide well the fit (dotted line) obtained with equation (1) is clearly not satisfactory and so the value of Γ_{LO} in table 2 is therefore in brackets. In fact, two different regimes are observed and for temperatures up to 150 K the FWHM of the transition remains unchanged, whereas for higher temperatures its dependence is similar to that of the 10.0 nm wide well. We believe that the two regimes correspond to a transition from the E^X_{HH}(1s–2s) $> h\nu_{LO}$ regime, where the exciton–LO phonon scattering is suppressed, to the E^X_{HH}(1s–2s) $< h\nu_{LO}$ regime, where exciton ionization occurs. The changeover is due to the inhomogeneous broadening of the 1s exciton levels and happens when delocalization, possibly through scattering with acoustic phonons, becomes effective. Although E^X_{HH}(1s–2s) $> h\nu_{LO}$ holds for individual states, the line widths are defined by the spatial extent of the excitons and this condition is not met by exciton levels broadened by $\sim$10 meV after delocalization.

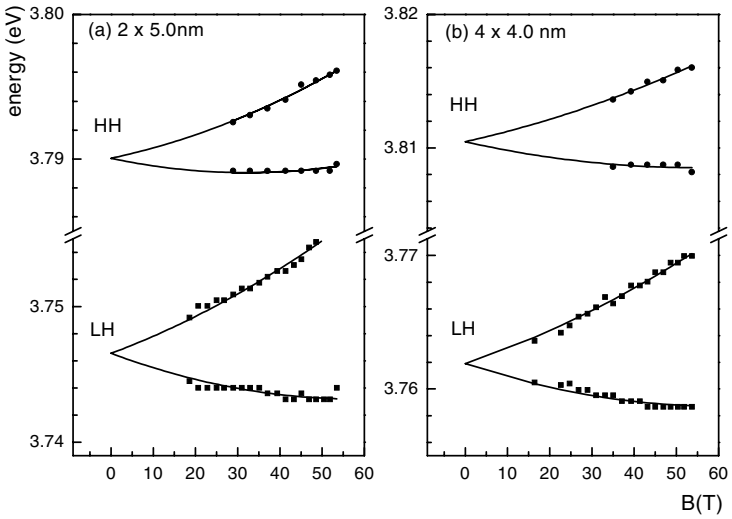

Figure 8. Measured transition energies for light (LH) and heavy hole (HH) exciton transitions for the 5.0 nm and 4.0 nm ZnS quantum wells. Solid lines are the fit obtained with equation (2).

5. Magneto-optics of ZnS

In the case of zincblende ZnS the bulk exciton binding energy is 36 meV and the LO phonon energy is 44 meV. Thus, in a practical quantum well structure where the exciton binding energy can typically be enhanced by a factor of two, it is clear that the condition $E_{1s\rightarrow 2s} > h\nu_{LO}$ can easily be satisfied. Magneto-reflectivity experiments were carried out in pulsed magnetic fields. The samples were immersed in liquid helium (4 K) in the bore of a resistive magnet through which was passed the energy stored in a 8 μF bank of capacitors, charged up to ~5000 V, inducing fields of up to 55 T. A xenon flash lamp was used as a white light source and the signal was detected with a CCD camera in 1 ms. Although higher excited exciton states were not clearly observed during the experiments, much information is obtained from the analysis of the magnetic field dependence of the ground states of the exciton transitions. The exciton g-factors for the light hole (LH) and HH excitons were measured for different well widths and the diamagnetic shift was obtained as a function of well width. The experimental values are in good agreement with our calculations and from the diamagnetic shift for each quantum well values for the exciton binding energies are deduced.

The spin degeneracy of the ground state transitions at zero magnetic field is lifted and an energy splitting is observed with increasing magnetic field for samples with quantum well widths from 3.5 to 10.0 nm thick. Figure 8 shows the ground state transitions for HH and LH as a function of the applied field for the 5.0 nm and 4.0 nm wide ZnS quantum wells. The exchange interaction of the quantum well ground state transitions is assumed to be negligible, as no level anticrossing was observed. Ideally, experiments with circularly polarized light in magnetic fields up to 20 T should be carried out to confirm this assumption.

As previously reported by Puls *et al* [24] the ground state transition energies can be described by a sum of zero-field energy, diamagnetic shift and Zeeman splitting:

$$E(B) = E_i + \delta B^2 \pm \tfrac{1}{2} g_{eff} \mu_B B \qquad (2)$$

Table 3. Effective exciton g-factors and diamagnetic parameters for heavy and light hole excitons in ZnS quantum wells.

Well width (nm)	g_{eff}(HH)	δ(HH) (μ eV T^{-2})	g_{eff}(LH)	δ(LH) (μ eV T^{-2})
3.5	—	—	4.22	0.50
4.0	2.45	0.65	3.67	0.89
5.0	2.14	0.96	4.01	1.00
10.0	3.48	1.56	4.10	1.55

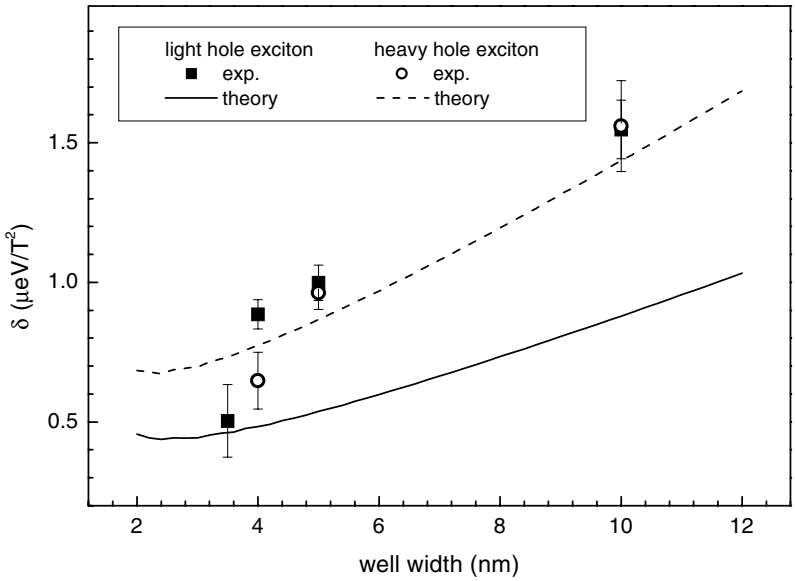

Figure 9. Measured values for diamagnetic parameter δ for LH (■), HH (○) excitons. Calculated values for LH (solid curve) and HH excitons (dashed curve).

where E_i stands for the E1LH1 or E1HH1 transitions at zero field, δ is the diamagnetic parameter and μ_B is the Bohr magneton.

The effective exciton g-values measured for both LH and HH excitons are summarized in table 3. The effective g-values for the HH are smaller than for the LH for the range of well widths investigated. Considering an effective g-value of 1.88 for the conduction band electrons in unstrained bulk ZnS, the measured LH exciton g-values indicate that the Zeeman effects of holes and electrons do not cancel each other out but are additive. The situation is different for the HH exciton, where the contributions of the HH and conduction band electrons partially cancel each other out.

The diamagnetic shift was measured for the LH and HH excitons for quantum well widths of 3.5 to 10.0 nm and 4.0 to 10.0 nm, respectively. The diamagnetic parameter δ is a measure of the carrier confinement; decreasing values of δ are expected for increasing confinement and indeed this trend could be experimentally verified for both types of exciton in the samples investigated, as can be seen in figure 9. The diamagnetic shift in weak magnetic fields of $\gamma < 0.4$, corresponding to 52 T for ZnS, can be calculated by first order perturbation

Table 4. ZnS heavy and light hole exciton binding energies obtained by fitting the magnetic field dependence; note $h\nu_{LO} = 44$ meV.

Well width (nm)	$E^X_{HH}(1s-2s)$ (meV)	$E^X_{HH}(1s-2s)$ (meV)	$E^X_{HH}(1s-2s)$ (meV)	$E^X_{HH}(1s-2s)$ (meV)
3.5	—	—	47.4	57.8
4.0	48.0	58.5	34.1	43.6
5.0	38.2	48.0	31.7	41.0
10.0	28.6	37.7	24.2	33.0

theory [28]:

$$\Delta E_{dia} = \delta B^2 = \frac{e^2 B^2}{8\mu_{xy}} \langle \rho^2 \rangle \tag{3}$$

where μ_{xy} is the in-plane reduced exciton mass and ρ is the in-plane radius. The spatial extension of an exciton reaches its minimum for maximum confinement and so the value of $\langle \rho^2 \rangle$ is expected to decrease with decreasing quantum well width until maximum confinement is reached. For even narrower wells, the value of $\langle \rho^2 \rangle$ increases again, as tunnelling effects become important. For bulk the relation $\langle \rho^2 \rangle = 2a_B^2$ holds, whereas for purely 2D excitons $\langle \rho^2 \rangle = \frac{3}{8} a_B^2$, where a_B is the bulk Bohr radius. As a first approximation, the binding energies for both LH and HH excitons were calculated and then the corresponding Bohr radii $a_{B(Q2D)}$ were used for calculating the diamagnetic shift with (3) assuming

$$\langle \rho^2 \rangle = 2a^2_{B(Q2D)}. \tag{4}$$

Exciton binding energies deduced by using the above approximation are given in table 4. The values for $E^X(1s–2s)$ were obtained from the 1s values by applying an analytical formula given Mathieu *et al* [29]. These first results indicate that $E^X(1s–2s) > h\nu_{LO}$ is achievable for heavy and light hole excitons for quantum wells narrower than 4 nm.

6. Conclusions

In conclusion, we have measured the exciton binding energies for two samples with different ZnSe well widths in MgS barriers. The value of 43.9 meV obtained for the narrow well is the largest value reported for this material system. Due to the absence of final states of scattering, the broadening of the transitions due to LO phonon scattering in this sample should be diminished compared with the wider quantum well samples. In fact, the value of the FWHM of the HH exciton for the 5.0 nm quantum well is constant up to 150 K indicating a strong decrease of the exciton–LO phonon scattering process in this regime.

Reflectivity and magneto-optics were used to study the excitonic properties of high quality ZnS quantum wells in ZnMgS. Heavy and light hole exciton transitions as narrow as 5 meV are observed for quantum wells with thicknesses ranging from 3.5 to 10.0 nm. The magnetic field dependences of the LH and HH transitions are described as a sum of the Zeeman effect and a diamagnetic shift. The small diamagnetic shift for the 3.5 and 4.0 nm quantum wells indicates the strong carrier confinement in these samples. The corresponding exciton binding energies indicate that for quantum wells narrower than 4.0 nm the exciton–LO phonon scattering can be suppressed for both light and heavy hole excitons.

Acknowledgments

We would like to thank Dr I Galbraith for valuable discussions. We gratefully acknowledge the support of EPSRC and the ESPRIT EU program. CM is grateful for the support of the Société des Amis des Sciences and the EU through its TMR scheme.

References

[1] Uenoyama T 1995 *Phys. Rev.* B **51** 10 228
[2] Kreller F, Puls J and Henneberger F 1996 *Appl. Phys. Lett.* **69** 2406
[3] Nojima S 1992 *Phys. Rev.* B **46** 2302
[4] Toyozawa Y and Hermanson J 1968 *Phys. Rev. Lett.* **21** 1637
[5] Itoh T, Nishijima M, Ekimov A I, Gourdon C, Efros Al L and Rosen M 1995 *Phys. Rev. Lett.* **74** 1645
[6] Zimin L, Nair S V and Masumoto Y 1998 *Phys. Rev. Lett.* **80** 3105
[7] Pelekanos N T, Haas H, Magnea N, Belitsky V I and Cantarero A 1997 *Phys. Rev.* B **56** 10 056
[8] Teraguchi N, Mouri H, Tomomura Y, Suzuki A, Taniguchi H, Rorison J and Duggan G 1995 *Appl. Phys. Lett.* **67** 2945
[9] Uesugi K, Obinata T, Kumano H, Nakahara J and Suemune I 1996 *Appl. Phys. Lett.* **68** 844
[10] Nashiki H, Suemune I, Kumano H, Suzuki H, Obinata T, Uesugi K and Nakahara J 1997 *Appl. Phys. Lett.* **70** 2350
[11] Kumano H, Nashiki H, Suemune I, Arita M, Obinata T, Suzuki H, Uesugi K and Nakahara J 1997 *Phys. Rev.* B **55** 4449
[12] Suemune I, Uesugi K, Suzuki H, Nashiki H and Arita M 1997 *Phys. Status Solidi* b **202** 845
[13] Okuyama H, Nakano K, Miyajima T and Akimoto K 1991 *Japan. J. Appl. Phys.* **30** L1620
[14] Okuyama H, Kishita Y and Ishibashi A 1998 *Phys. Rev.* B **57** 2257
[15] Bradford C, O'Donnell C B, Urbaszek B, Balocchi A, Morhain C, Prior K A and Cavenett B C 2000 *Appl. Phys. Lett.* **76** 3929
[16] Ozanyan K B, May L, Nicholls J E, Hogg J H C, Hagston W E, Lunn B and Ashenford D E 1996 *J. Cryst. Growth* **159** 89
[17] Ichino K, Akiyoshi S, Kawakami T, Misasa H, Kitagawa M and Kobayashi H 1997 *Japan. J. Appl. Phys.* **36** L1283
[18] Ichino K, Ueyama K, Yamamoto M, Kariya H, Miyata H, Misasa H, Kitagawa M and Kobayashi H 2000 *J. Appl. Phys.* **87** 4249
[19] Ichino K, Kariya H, Suzuki N, Ueyama K, Kitagawa M and Kobayashi H 2000 *J. Cryst. Growth* **214/215** 135
[20] Telfer S A, Morhain C, Urbaszek B, O'Donnell C, Tomasini P, Balocchi A, Prior K A and Cavenett B C 2000 *J. Cryst. Growth* **214/215** 197
[21] Tapfer L and Ploog K 1989 *Phys. Rev.* B **40** 9802
[22] Tanner B K 1993 *J. Phys. D: Appl. Phys.* **26** A151
[23] Bradford C, O'Donnell C B, Urbaszek B, Balocchi A, Morhain C, Prior K A and Cavenett B C 2000 *Appl. Phys. Lett.* **76** 3929
[24] Puls J, Rossin V V, Henneberger F and Zimmermann R 1996 *Phys. Rev.* B **54** 4974
[25] Engbring J and Zimmermann R 1992 *Phys. Status Solidi* b **173** 733
[26] Blewett I J, Bain D J, Tookey A, Brown G, Galbraith I, Kar A K, Vögele B, Prior K A, Cavenett B C and Wherrett B S 1999 *Phys. Rev.* B **59** 9756
[27] Pelekanos N T, Ding J, Hagerott M, Nurmikko A V, Luo H, Samarth N and Furdyna J K 1992 *Phys. Rev.* B **45** 6037
[28] Oettinger K, Efros Al L, Meyer B K, Woelk C and Brugger H 1995 *Phys. Rev.* B **52** R5531
[29] Mathieu H, Lefevre P and Christol P 1992 *Phys. Rev.* B **46** 4092